

Discrimination of Single Base Substitutions in a DNA Strand Immobilized in a Biological Nanopore

Robert F. Purnell and Jacob J. Schmidt*

Department of Bioengineering, University of California, Los Angeles, California 90095

In resistive pulse sensing, modulations of ionic current flowing through an electrolyte-filled channel are used to identify and characterize objects passing through the channel. Detection of polynucleotides translocating through a nanopore channel¹ inspired further research into nanopore-based DNA analysis, with the goal of developing a rapid and inexpensive DNA sequencing technology.^{2–8} Initial work measuring free translocation of single-stranded DNA (ssDNA) and RNA measured reductions in current of which the magnitude and duration were sensitive to base composition, but the speed of translocation ($1–20 \mu\text{s}/\text{base}$)^{1–3,5,6} precluded resolution of individual bases as a result of the high measurement bandwidth and noise.

These bandwidths were significantly decreased by immobilizing the ssDNA within the pore through engineering of a “stopper” which cannot pass through the pore, such as a terminal hairpin,^{9–11} short complementary hybridized oligomer,^{12,13} or binding of a larger molecule (e.g., streptavidin^{12–16} or DNA polymerase¹³). Using streptavidin-terminated ssDNA, we previously measured distinct blockade current signals from polyhomonucleotides of adenine (A), cytosine (C), and thymine (T) and showed that each of these was distinguishable in both the 3′ leading or 5′ leading orientations.¹⁶

Here we describe an extension of this technique to measurements of blockade currents arising from immobilized polythymine (polyT) in which single bases of A, C, and G were substituted at 12 consecutive positions. The results of our measurements are complementary to a recently published study in which blockade currents of immobilized polyC strands containing single adenine substitutions were measured.¹⁵ As our

ABSTRACT Nanopores have been explored as highly sensitive sensors for detection and rapid sequencing of single molecules of DNA. To sequence DNA with a nanopore requires that adenine (A), cytosine (C), thymine (T), and guanine (G) produce distinct current signals as they traverse the pore. Recently, we demonstrated that homopolymers of adenine, cytosine, and thymine immobilized in the nanopore protein α -hemolysin (α HL) produced distinct current blockades dependent on their chemical orientation. To probe the detection limit of α HL, we examined immobilized single strands of T₄₀ DNA (polyT) with single base substitutions of A, C, and G at 12 positions on the strand occupying the stem region of α HL. We find blockade currents sensitive to base identity over most of these positions with the most sensitive region near the pore constriction. Adenine substitutions increase the measured blockade current to values intermediate to the polyT and polyA currents at a number of positions, while C substitutions increase the current to a level intermediate to polyT and polyC values in some positions, but decrease it below polyT in others. These changes in blockade current were also observed for G substitutions. These results indicate that total blockade currents measured in α HL arise from nucleotides at multiple locations and thus are not uniquely attributable to an individual base in a specific position, a finding consistent with a recently published study. The measurements of C and G substitutions also suggest that blockade current may be modulated through interactions between nucleotides and the pore interior at multiple sites in α HL.

KEYWORDS: DNA · nanopore · α -hemolysin · sensing · single molecule

analysis here focuses exclusively on single-stranded homopolymers of polyT with single nucleotide substitutions of A, C, and G with biotin on the 3′ end, we will refer to substituted strands by the identity of the substituted nucleotide and its position from the 3′ end. For example, S3′-T₉A₁T₃₀-5′, S3′-T₉C₁T₃₀-5′, and S3′-T₉G₁T₃₀-5′ (S = streptavidin) are called polyT_{A,10}, polyT_{C,10}, and polyT_{G,10}, respectively. We chose to position the biotin group on the 3′ end and to use polyT for the “background” because the 5′ leading orientation produced the largest separation between polyA, polyC, and polyT blockade currents in our previous study.¹⁶ Figure 1 shows a schematic of an immobilized ssDNA strand with a single base substituted (red bead) in a polyT strand (gray beads). We examined nucleotides substituted at positions 6 through 17. Assuming a biotin linker length

*Address correspondence to schmidt@seas.ucla.edu.

Received for review May 1, 2009 and accepted August 12, 2009.

Published online August 20, 2009.
10.1021/nn900441x CCC: \$40.75

© 2009 American Chemical Society

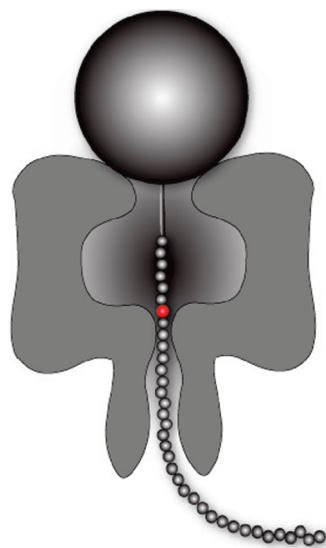


Figure 1. Schematic diagram of singly substituted polyT ssDNA immobilized in an α HL pore (roughly to scale). The streptavidin and biotin linker are idealized as a large silver sphere and a straight line attached to the ssDNA. The T bases are shown as small silver beads with the substituted base at position 7, colored red.

of 2 nm (IDTDNA, personal communication) and an interphosphate distance of ≈ 0.4 nm/base,¹⁷ positions 6–17 cover a 4.4 nm long section of the pore that includes the constriction and a significant portion of the stem.¹⁸

Applying the same voltage protocol described previously, we electrophoretically drove the ssDNA into the pore, measured the ionic current blockade (i_b), and ejected the strand, repeating the cycle thousands of times to obtain hundreds of immobilization events for each strand.¹⁶ Although previous work has demonstrated nonspecific binding of streptavidin to phosphatidyl-choline-containing lipid membranes,¹⁹ the repeatability of the blockade currents for single base substituted immobilized ssDNA (described below) indicates that the strand is fully drawn into the pore. Figure 2a shows a plot of i_b measured over the course of an experiment in which polyT, polyT_{A,10}, and polyT_{A,9} were sequentially added. As can be seen, when polyT_{A,10} was added to the solution, two sets of blockade current values are measured, with their frequency approximately corresponding to their stoichiometry. This suggests that the DNA is drawn into the pore from a random sample of DNA strands from the solution, rather than repeated sampling of the same strand. The histogram of these data (Figure 2b) was fit to a three-term Gaussian distribution with mean and standard deviation of 18.34 ± 0.06 , 19.32 ± 0.17 , and 19.76 ± 0.05 pA for polyT, polyT_{A,10}, and polyT_{A,9}, respectively. To quantify the sensitivity to single base substitutions in polyT, we subtracted the polyT i_b from the i_b for all substituted strands, producing a current deviation, Δi_b . From the distributions in Figure 2b, we obtained Δi_b of 0.97 ± 0.18 pA for polyT_{A,10} and 1.42 ± 0.08 pA for polyT_{A,9}. We repeated this experiment at least two times

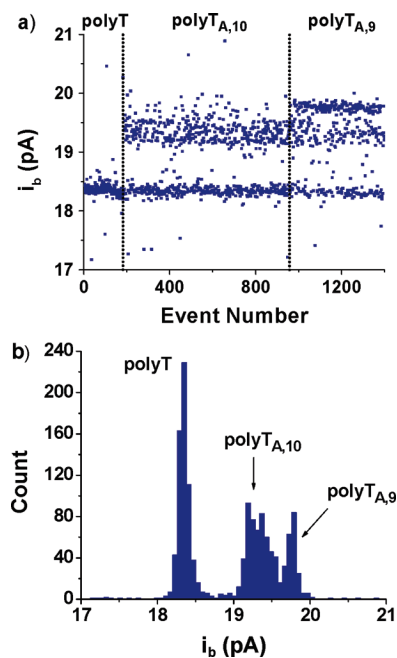


Figure 2. (a) Measurement of blockade currents from sequential addition of polyT and strands with single adenine bases substituted at positions 10 and 9, respectively, recorded at 120 mV. Additional strands were added without exchanging solutions to allow for direct comparison of blockade currents for substituted strands with polyT in identical solution conditions. Dotted lines depict the point at which a new strand was added to solution. (b) Histogram of data in (a) shows three distinct distributions of blockade current. Subtraction of the i_b of polyT from each distribution's peak i_b yielded a Δi_b value that was plotted in Figure 3, and the width of the distribution is reflected in its error bar there.

for each strand, adding 3–6 strands at a time for polyT_{A,6} through polyT_{A,17}, finding Δi_b for each strand.

If the addition of a new strand did not result in a measurably different current, then another experiment was performed in which the substituted strand was added after polyT to determine if i_b from that strand matched polyT or the i_b from another strand. Strands added after polyT that did not produce a measurably distinct blockade current were assigned Δi_b values of zero. The Δi_b was seen to remain constant across experiments in which the i_b of polyT itself varied by up to 1–2 pA. Infrequently measured slight linear drifts in the current signal ≤ 1 pA were corrected by fitting the polyT signal to a line and subtracting that trend from the data. These drifts are most likely due to evaporation of the solution, which would increase the electrolyte concentration during the 4–6 h duration of the experiment. The effect of this drift on Δi_b was negligible (see Supporting Information). Immobilization events that could not be cleared with negative voltage or included abrupt shifts (0–1 pA) in current were rare and not included in the analysis.

RESULTS AND DISCUSSION

The measured i_b for substitutions over positions 6–17 are compared to polyT in Figure 3 (left). The i_b of

polyT_{A,6} was found to be the same as i_b for the polyT reference (black line at $\Delta i_b = 0$) and is represented as a point on the polyT line. Substitution of A at positions 7–12 produced Δi_b values greater than 0 but less than the Δi_b for polyA (green line in Figure 3, from ref 14). The two points at position 8 represent an i_b distribution with two peaks, while the larger error bars at position 10 are indicative of broader distributions that were repeatable in several experiments (e.g., polyT_{A,10} in Figure 2b). For A substitutions, Δi_b reaches a maximum at position 9 and falls to 0 after position 12. Measurements were repeated at least twice for all substitution sites and all bases. The Δi_b values from individual experiments, along with i_b and i_{or} , and temperature and conductivity of the electrolyte are included in the Supporting Information.

We repeated this analysis for strands with C and G substitutions at positions 6–17. Figure 3 (center) shows a graph of Δi_b for C substitutions, with a blue line for the Δi_b of polyC for comparison.¹⁶ C substitutions produced i_b identical to polyT at positions 6 and 7 and above polyT at positions 8–10, with a peak at position 9, similar to A. PolyT_{C,11} strands produced signals predominantly below polyT (negative Δi_b), while signals above polyT were rare (data not shown). For substitutions at positions 12 through 17, Δi_b progressively increased to 0 pA at positions 15 and 16 and to 0.28 pA at position 17.

Blockade currents measured from G-substituted polyT strands were somewhat similar to those measured with C-substituted strands, as seen in Figure 3 (right). A polyG reference line could not be measured because long polyG strands cannot be readily synthesized (IDTDNA, communication) due to formation of secondary structure.²⁰ As with C, Δi_b values started at 0 for positions 6 and 7 and increased for polyT_{G,8} and polyT_{G,9}. However, after position 9, there were some differences observed for G-substituted strands: polyT_{G,10} produced an i_b distribution with two peaks below the polyT i_b , and polyT_{G,11} produced a two-peaked distribution with values very close to polyT (also see Supporting Information). PolyT_{G,12} produced a positive Δi_b , while substitution at positions 13 and 14 was the same as the polyT baseline. Interestingly, G substitutions at positions 15 and 16 produced large positive Δi_b values, while position 17 yielded a negative Δi_b . Average Δi_b values and data from individual experiments for G substitutions are included in the Supporting Information.

Previously, we found that polyA, polyC, and polyT produced unique blockade currents when immobilized in α HL with both 3' and 5' ends inserted into the pore.¹⁶ PolyT in the 5' leading orientation serves as a good reference strand, as it produces a smaller blockade current than polyC and polyA. If we view the total current measured when ssDNA is immobilized in the pore from a resistive pulse sensing perspective, we may expect that it is determined by the total resistance, which is the

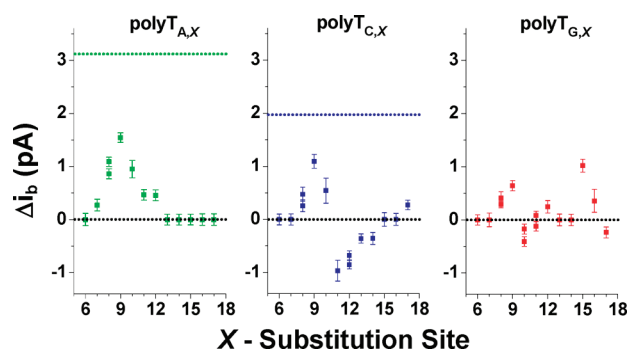


Figure 3. Graph of Δi_b for A, C, and G substitutions in a polyT strand at positions 6–17. The Δi_b values were obtained by subtracting the average i_b of polyT from the average i_b for each single base substituted strand. The averages of the Δi_b from several experiments for each base and substitution site are displayed in the graph with typical Δi_b values for polyA (green line) and polyC (blue line). The black dotted line represents the defined $\Delta i_b = 0$ for polyT. For several substitution sites, the histogram of i_b contained two peaks or one broad single peak. For two-peaked distributions (e.g., $X = 8$, for A, C, and G), two distinct points represent the two peak i_b values in the histogram. Broader distributions (e.g., $X = 10$ for A (left panel) and C (center panel)) are represented by points with larger error bars, which represent the combined standard deviations in Δi_b for all experiments. These characteristic distributions were repeatable in all experiments.

sum of the resistances of each section of the pore and the nucleotide contained within it. As a result, since the blockade current for polyA and polyC is greater than that for polyT, one may expect that substitution of a single A or C would either increase the measured blockade current or produce no change at all. Further, if α HL has a single sense region, this change would occur only for strands with substitutions in that one position or near it.

Blockade currents for polyT strands with A substitutions suggest a single recognition region in α HL. Non-zero Δi_b values were observed for $X = 7$ –12, with a peak at $X = 9$, while nucleotide substitutions outside this location ($X = 6$ and $X > 12$, along with 3'-C₅T₃₅-5' (data not shown)) yielded Δi_b of 0. Using the polyT strand as a 0.4 nm/base ruler¹⁷ and accounting for the ≈ 2 nm biotin–ssDNA linker length (IDTDNA, communication), we estimate positions 7–12 are approximately 4.8–6.8 nm from the streptavidin, corresponding with the constriction of the pore, where the diameter reaches a minimum of 1.4 nm.²¹ From this, we conclude the constriction of the pore forms a recognition site. Stoddart *et al.* found a qualitatively similar trend in blockade currents measured in wild type α HL for A substitutions in polyC at $X = 7$ –12, with maximal differences of the normalized blockade current at $X = 8$ and 9. Quantitative agreement with that work was not obtained, possibly due to the different applied voltages (160 mV in their work vs 120 mV here) and the background polyhomonucleotide polyC, which produces a residual current signal $\approx 1\%$ larger than polyT.¹⁶ Although we measured $\Delta i_b = 0$ for all $X > 12$, Stoddart *et al.* reported two additional recognition regions for polyC strands with A substitutions at $X > 12$, with maxi-

mum sensitivities at $X = 14$ (where $\Delta i_b > 0$) and $X = 18$ (where $\Delta i_b < 0$).¹⁵

Evidently, the “background” homopolymer plays a major role in the observed differences in the measured currents for A substitutions for $X > 12$, demonstrating that nucleotides at multiple sites in an immobilized strand are important determinants of blockade current. One possible source of the differences is the contrasting secondary structures of polyC and polyT. PolyC forms a tight helix as a result of base stacking and hydrogen bonding between adjacent pyrimidines.^{22,23} In contrast, studies on thymidylate dimers predict an unstacked structure for polyT that more closely resembles a freely jointed chain, where nucleotides are not capable of base stacking.²² Since the scanning of adenine through a polynucleotide strand effectively introduces a defect into the strand, the substitution of a single base could have a different affect on the unique secondary structures of polyT and polyC. Another hypothesis related to this is that, since the bases in polyC’s helix hydrogen bond with each other, the presence of adenine may disrupt these hydrogen bonds, leaving the cytosines on either side of the adenine able to hydrogen bond with amino acid side chains in the pore. Thus, not only adenine but also the “edges” of the cytosine helix are being scanned. In this way, if we attribute the recognition sites we observe at $X > 12$ for C and G to interactions between C and G and the pore wall, the cytosine edges could also participate in these interactions. Glycine has shown a higher affinity to form single hydrogen bonds with cytosine and guanine *versus* thymine and adenine;²⁴ the center of the α HL pore interior is glycine-rich.²¹

This point is further supported by a similar examination of the sequential substitution of G and C within polyT. Figure 3 (center and right) shows at least three recognition sites in the pore for G and C substitutions in polyT, represented by several local extrema in Δi_b . The first recognition site for G and C substitutions, located around $X = 9$, appears to be the same as that measured for A substitutions, suggesting that a structural aspect of the pore (the constriction) provides sensitivity to nucleotide identity. Further down the pore, Δi_b of C substitutions decreased from their peak value at position 9 to ultimately produce negative Δi_b values at $X = 11–14$, a particularly interesting result, given that the blockade current of polyC is greater than that of polyT. In this same spanned length, G substitutions were slightly negative at $X = 10$ but slightly positive at $X = 11$ (or negative, see Supporting Information) and $X = 12$. G substitution at position 15 gave its largest Δi_b , although the Δi_b measured for C and A at the same position was 0. The difference seen in these measurements, together with the $\Delta i_b = 0$ of A substitutions over the same region, suggests a base-specific interaction with the pore as a determinant of the measured blockade current in these regions, in contrast to the re-

gion at $X = 9$. We can also understand the measured negative Δi_b for scanned C by noting that the positive Δi_b of polyC cannot be directly compared to the Δi_b of a scanned single base because the base-stacked polyC interacts minimally with the pore, whereas the single C is much freer to interact and produce different blockade currents.

Although Stoddart *et al.* did not report scans of T and G through the polyC strand, they did report measurements of blockade currents for all four bases at $X = 9, 14, \text{ and } 18$. At $X = 9$, blockade currents in decreasing order were A, C, and finally T and G being indistinguishable. In contrast, we find the Δi_b for all four bases to be distinguishable at this position with A, C, G, and T in decreasing order. Stoddart also found that at $X = 14$ all four bases are distinguishable, with the decreasing order of current G, A, T, and C. We find at that position A, T, and G give the same Δi_b ($\Delta i_b = 0$) and that of C is slightly negative. Although Stoddart’s larger voltage would give rise to a larger electric field, possibly stretching the DNA more than in our experiment, we measure the same values of Δi_b at $X = 13$. Together with our measurement of $\Delta i_b = 0$ for A substitutions for $X > 12$, these results suggest that there is a qualitative difference in our systems, as seen from blockade currents for $X > 12$, arising from the applied voltage or the different polynucleotide used.

In this study, distributions of measured blockade currents, characterized by one or two peaks and the distribution width, are highly sensitive to the identity and position of the substituted nucleotide. In previous homopolymer studies, multiple peaks in the i_b histogram were attributed to chemically different molecules or different orientations of identical molecules.^{10,16} Similarly, one might attribute the appearance of two peaks for all three nucleotides at $X = 8$ to a reduction in pore diameter, as nucleotides at or near that position could be constrained to two discrete orientations, while a broad distribution (*e.g.*, polyT_{C,10} and polyT_{A,10}) could represent a range of available positions. Examining the blockade current distributions at other positions, we find polyT_{G,10}, polyT_{G,11}, polyT_{C,12}, and polyT_{G,16} also produce distributions different from the other substituted nucleotides and substitution positions (see Figure 3). The difference in pore geometry at these locations ($X = 10$, constriction; $X = 16$, stem) and the fact that these trends were observed for both purines and pyrimidines at different sites (*e.g.*, A and C, but not G at position 10) suggest that distribution shapes may be influenced by nucleotide-specific interactions with the pore.

Full separation of the contribution of the scanned base and the background polynucleotide to the measured current may be obtainable if the bases in the background polynucleotide were replaced with abasic nucleotides. Our hypothesis of the dangling edges of the polyC helix interacting with the pore wall could also be explored by scanning A through an abasic strand

and comparing that to scans of AC, CA, and CAC through an abasic strand. The sensitivity of the measured current to nucleotide identity and interactions at a number of locations in the pore implies that, for ssDNA moving through the pore, the measured current would be a convolution of the DNA sequence at each position with the pore sensitivity as a function of position. Deconvolving these data could be made much

simpler if the pore's sensitive region were smaller and the remainder of the pore had no interaction with the resident ssDNA. For example, the MspA protein pore, with its small constriction region, has been explored as an alternative to α HL²⁵ because its potential for sensitivity to nucleotide identity at a smaller number of positions could simplify interpretation of measured blockade currents.

METHODS

Nanopore Methods: Lipid bilayer membranes containing α HL nanopores were created using methods previously described. Briefly, a 3% w/v solution of DPhPc (Avanti Polar Lipids) in *n*-decane (Sigma) was spread across a 100 μ m orifice in a Teflon partition. Self-assembly of the α HL nanopore into the membrane produced an instantaneous increase in conductance to \sim 1 nS. To capture, measure, and eject individual ssDNA strands for analysis, we applied alternating cycles of +120 and $-$ 100 mV for 4 and 1 s, respectively, using a custom voltage protocol (Pclamp, Molecular Devices, Sunnyvale, CA). The resultant current was amplified using a bilayer amplifier and headstage (BC-535, Warner Instruments, Hamden, CT) and acquired at 5 kHz.

DNA Samples: Single-stranded DNA (Integrated DNA Technologies, Coralville, IA) samples were dissolved in TE buffer (10 mM Tris, 1 mM EDTA, pH 7.5) at a concentration of 100 μ M and mixed in a 1:5 volume ratio with a KCl buffer solution (1 M KCl, 10 mM Tris HCl/1 mM EDTA) containing 16.7 μ M streptavidin (Sigma). After incorporation of a single channel and exchange of the buffer solution, the solution of streptavidin-linked ssDNA was added to the cis side of the chamber. To maintain the same fluidic volume, an identical amount of mixed fluid was then removed.

Acknowledgment. We thank S. Cheley for the kind donation of α HL. Funding was provided by NSF CAREER (0644442).

Supporting Information Available: Tables with Δi_b values from each experiment and corresponding experimental conditions, a discussion of blockade currents for polyT_{G,11}, corrections for drift in blockade current in a sample experiment, and the method used to estimate the number of immobilization events for each strand in each experiment. This material is available free of charge via the Internet at <http://pubs.acs.org>.

REFERENCES AND NOTES

- Kasianowicz, J. J.; Brandin, E.; Branton, D.; Deamer, D. W. Characterization of Individual Polynucleotide Molecules Using a Membrane Channel. *Proc. Natl. Acad. Sci. U.S.A.* **1996**, *93*, 13770–13773.
- Meller, A.; Nivon, L.; Branton, D. Voltage-Driven DNA Translocations through a Nanopore. *Phys. Rev. Lett.* **2001**, *86*, 3435–3438.
- Meller, A.; Nivon, L.; Brandin, E.; Golovchenko, J.; Branton, D. Rapid Nanopore Discrimination between Single Polynucleotide Molecules. *Proc. Natl. Acad. Sci. U.S.A.* **2000**, *97*, 1079–1084.
- Henrickson, S. E.; Misakian, M.; Robertson, B.; Kasianowicz, J. J. Driven DNA Transport into an Asymmetric Nanometer-Scale Pore. *Phys. Rev. Lett.* **2000**, *85*, 3057–3060.
- Folgoea, D.; Uplinger, J.; Thomas, B.; McNabb, D. S.; Li, J. L. Slowing DNA Translocation in a Solid-State Nanopore. *Nano Lett.* **2005**, *5*, 1734–1737.
- Deamer, D. W.; Branton, D. Characterization of Nucleic Acids by Nanopore Analysis. *Acc. Chem. Res.* **2002**, *35*, 817–825.
- Butler, T. Z.; Gundlach, J. H.; Troll, M. Ionic Current Blockades from DNA and RNA Molecules in the Alpha-Hemolysin Nanopore. *Biophys. J.* **2007**, *93*, 3229–3240.
- Akeson, M.; Branton, D.; Kasianowicz, J. J.; Brandin, E.; Deamer, D. W. Microsecond Time-Scale Discrimination among Polycytidylic Acid, Polyadenylic Acid, and Polyuridylic Acid as Homopolymers or as Segments within Single RNA Molecules. *Biophys. J.* **1999**, *77*, 3227–3233.
- Ashkenasy, N.; Sanchez-Quesada, J.; Bayley, H.; Ghadiri, M. R. Recognizing a Single Base in an Individual DNA Strand: A Step toward DNA Sequencing in Nanopores. *Angew. Chem., Int. Ed.* **2005**, *44*, 1401–1404.
- Mathe, J.; Aksimentiev, A.; Nelson, D. R.; Schulten, K.; Meller, A. Orientation Discrimination of Single-Stranded DNA Inside the Alpha-Hemolysin Membrane Channel. *Proc. Natl. Acad. Sci. U.S.A.* **2005**, *102*, 12377–12382.
- Sauer-Budge, A. F.; Nyamwanda, J. A.; Lubensky, D. K.; Branton, D. Unzipping Kinetics of Double-Stranded DNA in a Nanopore. *Phys. Rev. Lett.* **2003**, *90*, 238101.
- Nakane, J.; Wiggin, M.; Marziali, A. A Nanosensor for Transmembrane Capture and Identification of Single Nucleic Acid Molecules. *Biophys. J.* **2004**, *87*, 3618.
- Cockroft, S. L.; Chu, J.; Amorin, M.; Ghadiri, M. R. A Single-Molecule Nanopore Device Detects DNA Polymerase Activity with Single-Nucleotide Resolution. *J. Am. Chem. Soc.* **2008**, *130*, 818–820.
- Kasianowicz, J. J.; Henrickson, S. E.; Weetall, H. H.; Robertson, B. Simultaneous Multianalyte Detection with a Nanometer-Scale Pore. *Anal. Chem.* **2001**, *73*, 2268–2272.
- Stoddart, D.; Heron, A. J.; Mikhailova, E.; Maglia, G.; Bayley, H. Single-Nucleotide Discrimination in Immobilized DNA Oligonucleotides with a Biological Nanopore. *Proc. Natl. Acad. Sci. U.S.A.* **2009**, *106*, 7702–7707.
- Purnell, R. F.; Mehta, K. K.; Schmidt, J. J. Nucleotide Identification and Orientation Discrimination of DNA Homopolymers Immobilized in a Protein Nanopore. *Nano Lett.* **2008**, *8*, 3029–3034.
- Bustamante, C.; Smith, S. B.; Liphardt, J.; Smith, D. Single-Molecule Studies of DNA Mechanics. *Curr. Opin. Struct. Biol.* **2000**, *10*, 279–285.
- Song, L. Z.; Hobaugh, M. R.; Shustak, C.; Cheley, S.; Bayley, H.; Gouaux, J. E. Structure of Staphylococcal Alpha-Hemolysin, a Heptameric Transmembrane Pore. *Science* **1996**, *274*, 1859–1866.
- Chandler, E. L.; Smith, A. L.; Burden, L. M.; Kasianowicz, J. J.; Burden, D. L. Membrane Surface Dynamics of DNA-Threaded Nanopores Revealed by Simultaneous Single-Molecule Optical and Ensemble Electrical Recording. *Langmuir* **2004**, *20*, 898–905.
- Ralph, R. K.; Khorana, H. G.; Connors, W. J. Secondary Structure and Aggregation in Deoxyguanosine Oligonucleotides. *J. Am. Chem. Soc.* **1962**, *84*, 2265–2266.
- Movileanu, L.; Cheley, S.; Howorka, S.; Braha, O.; Bayley, H. Location of a Constriction in the Lumen of a Transmembrane Pore by Targeted Covalent Attachment of Polymer Molecules. *J. Gen. Physiol.* **2001**, *117*, 239–251.
- Adler, A.; Grossman, L.; Fasman, G. D. Single-Stranded Oligomers and Polymers of Cytidylic and 2'-Deoxycytidylic Acids—Comparative Optical Rotatory Studies. *Proc. Natl. Acad. Sci. U.S.A.* **1967**, *57*, 423-A.
- Bowling, J. M.; Bruner, K. L.; Cmarik, J. L.; Tibbetts, C. Neighboring Nucleotide Interactions During DNA Sequencing Gel-Electrophoresis. *Nucleic Acids Res.* **1991**, *19*, 3089–3097.

24. Luscombe, N. M.; Laskowski, R. A.; Thornton, J. M. Amino Acid–Base Interactions: A Three-Dimensional Analysis of Protein–DNA Interactions at an Atomic Level. *Nucleic Acids Res.* **2001**, *29*, 2860–2874.
25. Butler, T. Z.; Pavlenok, M.; Derrington, I. M.; Niederweis, M.; Gundlach, J. H. Single-Molecule DNA Detection with an Engineered MspA Protein Nanopore. *Proc. Natl. Acad. Sci. U.S.A.* **2008**, *105*, 20647–20652.